

Astronomy Letters, Vol. 31, No. 10, 2005, pp. 681-694. Translated from Pis'ma v Astronomicheskii Zhurnal, Vol. 31, No. 10, 2005, pp. 764-779. Original Russian Text Copyright © 2005 by Chelovekov, Lutovinov, Grebenev, Sunyaev.

Observations of the X-ray Burster MX 0836-42 by the INTEGRAL and RXTE Orbiting Observatories

I. V. Chelovekov^{1*}, A.A. Lutovinov¹, S.A. Grebenev¹, R.A. Sunyaev^{1,2}

¹ *Space Research Institute, Russian Academy of Sciences, Profsoyuznaya ul. 84/32, Moscow, 117810 Russia*

² *Max-Planck-Institut für Astrophysik, Karl-Schwarzschild-Str. 1, Postfach 1317, D-85741 Garching, Germany*

Abstract. We present the results of our study of the emission from the transient burster MX 0836-42 using its observations by the INTEGRAL and RXTE X-ray and gamma-ray observatories in the period 2003-2004. The source's broadband X-ray spectrum in the energy range 3-120 keV has been obtained and investigated for the first time. We have detected 39 X-ray bursts from this source. Their analysis shows that the maximum 3-20 keV flux varies significantly from burst to burst, $F \sim (0.5 - 1.5) \times 10^{-8} \text{ erg cm}^{-2} \text{ s}^{-1}$. Using the flux at the maximum of the brightest detected burst, we determined an upper limit for the distance to the source, $D \simeq 8 \text{ kpc}$.

Key words: neutron stars – bursters, transients; X-ray sources – MX 0836-42.

* e-mail: chelovekov@hea.iki.rssi.ru

INTRODUCTION

The transient X-ray source MX 0836-42 was discovered in 1971 by the OSO-7 satellite (Markert et al. 1975). Its position almost coincided with the probable position of the point source detected in December 1970 and February 1971 by the UHURU observatory (Kellogg et al. 1971). Since the intensity of the latter was too low, it was not included in the official UHURU catalog of sources (Markert et al. 1977; Cominsky et al. 1978). In 1990, the WATCH all-sky X-ray monitor aboard the GRANAT orbiting observatory detected a bright transient source near MX 0836-42 (Sunyaev et al. 1990, 1991; Lapshov et al. 1992). Its 5-15 keV flux during these observations reached a level comparable to the flux from the Crab Nebula. The localization accuracy of the source was only 1° . Analysis of the ROSAT data revealed two point sources in this region spaced 24 arcmin apart (Hasinger et al. 1990). Subsequently, the presence of these two sources was confirmed by data from the ART-P telescope of the GRANAT observatory (Sunyaev 1991). Type-I X-ray bursts were detected from the northern source, which allows MX 0836-42 to be classified as a low-mass X-ray binary containing a neutron star with a weak magnetic field, while X-ray pulsations with a period of ~ 12 s were detected from the southern source GRS 0834-430, which characterize it as an X-ray pulsar (Makino 1990; Grebenev and Sunyaev 1991). Studies of the emission from MX 0836-42 showed that its energy spectrum could be described by a power law with a photon index of ~ 1.5 (Aoki et al. 1992). In this paper, based on the data obtained in 2003-2004 by the instruments of the INTEGRAL and RXTE orbiting observatories, we have constructed and analyzed the source's spectrum during X-ray bursts and for the first time persistent broadband spectrum in the energy range 3-120 keV. We discuss the properties of the detected X-ray bursts.

OBSERVATIONS AND DATA ANALYSIS

The INTEGRAL international orbiting gamma-ray observatory (Winkler et al. 2003) was placed in orbit by a Russian PROTON launcher on October 17, 2002 (Eismont et al. 2003). There are four instruments aboard the observatory: the SPI gamma-ray spectrometer, the IBIS gamma-ray telescope, the JEM-X X-ray monitor, and the OMC optical monitor. Here, we use the data obtained by the ISGRI detector, one (upper) of the two detectors of the IBIS gamma-ray telescope (Ubertini et al. 2003), and by the second module of the JEM-X X-ray monitor (Lund et al. 2003). The ISGRI/IBIS detector is sensitive to photons in the energy range 15-200 keV and has an energy resolution of $\sim 7\%$ at 100 keV. The IBIS telescope includes a coded mask that allows it to be used not only for spectral and timing analyses of the emission, but also for reconstructing the image of the sky in the $29^\circ \times 29^\circ$ field of view of the instrument (the fully coded field of view is $9^\circ \times 9^\circ$) with an angular resolution of 12 arcmin (FWHM) and localizing X-ray and gamma-ray sources to within 1-2 arcmin. The JEM-X telescope is also based on the principle of a coded aperture. It is sensitive to photons in the energy range 3-35 keV, and its fully coded field of view is $4^\circ.8$ in diameter.

We analyzed the JEM-X and IBIS data using the OSA 4.1 data processing software package distributed by the INTEGRAL Science Data Center (ISDC). To construct the light curves

and spectra for MX 0836-42, we used the fluxes that were obtained by reconstructing the image of the sky in the field of view of the instrument and identifying the observed sources. The photon spectrum of the source in 20-120 keV energy band was reconstructed using a 50-channel ISGRI/IBIS response matrix that was constructed from observations of the source in the Crab Nebula and that allows us to restore the spectral shape of the source to within 4% and the normalization to within 7%.

The RXTE observatory carries three main instruments: the PCA spectrometer based on five xenon proportional counters sensitive to photons in the energy range 2-60 keV, the HEXTE spectrometer sensitive to photons up to 200 keV, and the ASM all-sky monitor sensitive to photons in the energy range 2-12 keV. The RXTE observational data for the source under study were provided by the NASA archive (HEASARC). We used the LHEASOFT 5.3.1 software package and the XSPEC 11.3.1 code to process the PCA/RXTE and HEXTE/RXTE data and to analyze the source’s spectra.

The X-ray transient MX 0836-42 was within the IBIS/ISGRI field of view several times in the period from March 2003 through May 2004 (Table 1), within the framework of both the Core and Open observing programs (Winkler et al. 2003). The total exposure time for this source was more than 2.5 Ms. We used the data obtained when scanning the Galactic plane and during deep observations of a region near the source Vela X-1.

The most recent accessible observations of the above-mentioned Vela X-1 region were performed from June 12 through July 6 and from November 27 through December 11, 2003. The total JEM-X and IBIS exposure times for MX 0836-42 were ~ 0.73 and ~ 1.13 Ms for the former period and ~ 0.45 and ~ 1.0 Ms for the latter period, respectively. We used only the pointings during which the source under study was within the fully coded field of view of the instrument. This was done to avoid the inaccuracies in restoring the energy flux from the source under study as much as possible. The difference between the exposure times for the two instruments stems from the fact that the fully coded field of view of the JEM-X monitor is smaller than that of the IBIS telescope (see above).

Figure 1 shows the light curves of the source for the period 52650-53400 MJD constructed from the data of the ISGRI/IBIS (20-60 keV) and JEM-X (3-20 keV) telescopes aboard the INTEGRAL observatory and the ASM (2-12 keV) and PCA (3-20 keV) instruments aboard the RXTE observatory. Figure 2 presents the source’s light curve constructed from all of the available ASM/RXTE data. The fluxes shown are the ratios of the fluxes from MX 0836-42 to the flux from the Crab Nebula in the corresponding energy range.

During two of the three groups of measurements consisting of nine (52773-52825 MJD) and six (53186-53261 MJD) observations, respectively, present in Fig. 1a, the flux from the source under study was below the sensitivity threshold of the ISGRI detector. The upper limits on the flux from MX 0836-42 for each of these pointings are given at the 3σ level.

Figures 1b and 2 show the light curve for MX 0836-42 in the energy range 2-12 keV constructed from the ASM/RXTE data. Each point in the figure corresponds to the flux from the source averaged over a 36-ks period.

Table 2 presents information about the observations by the RXTE orbiting observatory in 2003-2004 during which MX 0836-42 was within the PCA and HEXTE fields of view. Figure 3b shows the 3-120 keV fluxes from this source determined by processing the RXTE (PCA+HEXTE) data. Here, we use only the sessions of stable pointings of the instruments at the source.

THE PERSISTENT SPECTRUM

Based on the INTEGRAL data, we were able to construct the 3-120 keV spectrum of the source under study (Fig. 4, dashes). For this purpose, we used the observational data obtained by the JEM-X X-ray monitor (3-20 keV; Fig. 1c, region II) and the ISGRI/IBIS detector (20-120 keV; Fig. 1a, region II) during 137-141 orbital cycles (Table 1, November 27 - December 9, 2003), when the source was in its high state and its flux in these energy ranges was $\sim 50 - 70$ mCrab. During the fitting, the JEM-X spectrum was renormalized to correspond to the normalization of the ISGRI/IBIS spectrum; the normalization factor was 1.15. We now attribute the spectral features in the regions 6-8, 12-15 and 20-25 keV to systematic measurement errors.

A spectral analysis of the emission from MX 0836-42 using the data averaged over each of the INTEGRAL orbital cycles mentioned above showed that the spectral shape of the source did not change significantly over this period. Therefore, we used the averaged data of these six orbital cycles (Fig. 1a, region II) to construct and analyze the broadband spectrum. Fitting the constructed spectrum of the source by a power law with a high energy exponential cutoff yields a photon index of $\alpha = 1.46 \pm 0.08$ and a cutoff energy of $E_{cut} = 51.1 \pm 1.4$; the 3-120 keV flux from the source was $F = (2.29 \pm 0.10) \times 10^{-9} \text{ erg cm}^{-2} \text{ s}^{-1}$.

Based on the ISGRI/IBIS data averaged over 55-58 (Fig. 1a, region I) and 149-194 (Fig. 1a, region III) orbital cycles, we constructed the source's spectra only in the energy range 20-60 keV, since the total exposure times in these regions were only ~ 20 and ~ 50 ks, respectively, which are much shorter than the exposure time in region II (~ 1 Ms). The statistical significance of the source's detection at energies above 60 keV during these observations was insufficient to construct a qualitative spectrum. Fitting these spectra by a power law with a high-energy exponential cutoff yields a photon index $\alpha = 1.29 \pm 0.17$ for the former and $\alpha = 1.31 \pm 0.14$ for the latter (E_{cut} during these fitting was fixed at 50 keV).

Figure 4 (solid lines) shows examples of the spectra for MX 0836-42 that were obtained from the PCA (3-20 keV) and HEXTE (20-60 keV) data averaged over several successive pointings (the total exposure time is $\sim (2.9 - 10.5)$ ks). All of the spectra obtained were fitted in the energy range 3-60 keV by a power law with a high energy exponential cutoff. We also added the reflection of radiation from the accretion disk, the photoabsorption under the assumption of solar heavy-element abundances in the interstellar medium, and the fluorescence iron line at $E_{Fe} = 6.4$ keV to this model, which allowed the quality of the fit to be improved considerably (the χ^2 value per degree of freedom decreased from $\sim (8 - 10)$ to $\sim (1 - 2)$). In view of the uncertainty in the normalization of the HEXTE spectra, all of them were

multiplied by a constant to be renormalized to the level of the PCA spectra obtained during the same observation.

Table 3 presents the fitting results and the model fluxes corrected for the dead time of the detector and the HEXTE spectral normalization constants mentioned above. Figure 3 shows the time dependences of the photon index, the source’s persistent model flux, and the hydrogen column density (N_H) derived when fitting the spectra. The dotted line in this figure highlights the parameters determined from the data of January 29₁ and 31₂ (the subscript indicates the number of a given pointing among the pointings at the source on this day) and February 2, 2003. The relatively high values of N_H and the low values of the photon index and the flux obtained when fitting these data allow us to separate them into a group of observations with strong absorption. The derived mean photon index of the source’s power-law spectrum, $\sim (1.4 - 1.5)$, and the interstellar absorption, $\sim 3 \times 10^{22} \text{ atoms cm}^{-2}$ (Fig. 3, without including the observations from the group with strong absorption mentioned above), are comparable to those obtained previously when studying this source (Aoki et al. 1992; Belloni et al. 1993).

The iron emission line at $E_{Fe} = 6.4 \text{ keV}$ was detected in all PCA spectra. Since the PCA spectral resolution is too low for the line profile to be studied in detail, we fixed the line parameters at $E_{Fe} = 6.4 \text{ keV}$ and $\delta E_{Fe} = 0.1 \text{ keV}$ when fitting the spectra. The line equivalent width in the spectra under consideration was 100-310 eV.

X-RAY BURSTS

When analyzing the JEM-X 3-20 keV light curves for MX 0836-42, we found 24 X-ray bursts (Table 4). The light curves of this source were constructed only for the period of its reliable detection above the background level from the data obtained during 137-141 and 146 orbital cycles (Fig. 1, region III; Table 1, November 27 - December 24, 2003).

There were no pointings containing more than one burst. The separation between the nearest of the neighboring bursts was $\sim 2 \text{ h}$, in good agreement with the burst recurrence period for this source estimated previously (Aoki et al. 1992).

To carry out a detailed analysis of the bursts from the source under study in the energy range 3-20 keV, we used the 25 observations of MX 0836-42 performed by the PCA detector of the RXTE orbiting observatory from January 24 through March 20, 2003, and from January 18 through January 26, 2004 (Table 2). We found 15 X-ray bursts in the light curves constructed from these data. The source’s radiation temperature during the decay of these bursts decreased (Fig. 5b), which is characteristic of type I X-ray bursts (Lewin and Joss 1981). Analysis of the observations during which the observatory was repointed revealed no new burst.

The burst flux from the source reached its maximum, on average, in 6-8 s (Fig. 5b) and then remained at the same level for 3-4 s during some of the bursts (Fig. 5c). Table 5 gives the burst durations and the exponential burst decay times. The burst duration was defined

as the ratio of the total energy released in the burst component of the emission from the burst onset time to the time the flux decreased to 10% of its maximum to the mean burst energy flux over this period. To calculate the exponential burst decay time, we fitted the burst profile by an exponential time dependence of the flux.

A characteristic feature of 80% of the X-ray bursts detected by the PCA spectrometer from MX 0836-42 is a more or less distinct double-peaked structure. An example of such a burst is shown in Fig. 5a. It is believed that a multi-peaked burst shape can result from the following: (i) expansion of the photosphere under the pressure of a near-Eddington flux and (ii) peculiarities of the thermonuclear burning. Since we found no statistically significant increase in the color radius of the emitting object at the time of the dip between the peaks (the 3-20 keV flux decreased by $\sim 15\%$), we can assume that the double-peaked structure of the burst in this case is not related to photospheric expansion, but could result from peculiarities of the thermonuclear burning in the source during the burst.

Interestingly, the maximum 3-20 keV flux from the source during the X-ray bursts detected by the PCA spectrometer ranged from $F \sim 1.5 \times 10^{-8} \text{ erg cm}^{-2} \text{ s}^{-1}$ (Fig. 5c) to $F \sim 0.5 \times 10^{-8} \text{ erg cm}^{-2} \text{ s}^{-1}$ (Fig. 5d). This allows us to trace the dependence of this quantity on the total energy released during the burst (Fig. 6a). We see that the maximum burst flux rises with increasing total energy released during the burst. A similar dependence was found for other sources of X-ray bursts, such as 1608-522 (Murakami et al. 1980), 1728-337 (Basinska et al. 1984), 1735-44 (Lewin et al. 1980), and 1837+049 (Sztajno et al. 1983).

Since no photospheric expansion of the neutron star was reliably detected in any of the bursts studied, we used the flux at the maximum of the brightest of the X-ray bursts mentioned above (1.12 ± 0.24 Crab) to estimate the distance to MX 0836-42 by assuming that the source's luminosity at this time was close to the Eddington limit for a neutron star with a mass of $1.4 M_{\odot}$. The derived upper limit for the distance to the source is $D \sim 8$ kpc. This value is close to the lower limit for the distance to the source $D \sim (10 - 20)$ kpc estimated previously by Aoki et al. (1992) by assuming that the color radius of the emitting object during an X-ray burst would correspond to the neutron-star radius, 10 km.

Figures 5c and 5d show the time dependences of the model flux and the color temperature and radius of the emitting object obtained when fitting the source's spectra by a blackbody during the brightest and weakest bursts detected by the PCA/RXTE spectrometer. All of the spectra studied were corrected for the background count rate of the detector and the persistent emission from the source under study. The color temperature of the emitting region, on average, rose at the burst onset to 2-2.5 keV in 1-4 s and gradually fell to 1.5-2.0 keV during the burst. The color radius R_c of the emitting region, on average, rose at the burst onset from 1-3 to 4-6 km in 3-5 s and decreased insignificantly by the burst end (by $\sim 10 - 15\%$). This behavior of R_c may suggest that the size of the region affected by the explosion changes and that Comptonization plays a prominent role in shaping the spectrum. The mean values of the maximum temperature, $kT_{bb} \sim 2.5$ keV, and the radius, $R \sim (4-6) \times (D/8 \text{ kpc})$ km, are in good agreement with the values of these parameters obtained by Aoki et al. (1992).

Figure 6b shows the dependence of the persistent flux from the source on the total energy released during the burst constructed from the 15 X-ray bursts detected by the PCA/RXTE spectrometer. We see from this figure that there is a direct correlation between these quantities. This can serve as direct evidence for the current understanding of the burster phenomenon. Accreting matter falls to the neutron star surface in the time between bursts, releasing part of its gravitational energy in the form of radiation that we observe as the system’s persistent emission. Subsequently, this matter becomes a fuel for stable and explosive thermonuclear reactions, the latter of which are observed as an X-ray burst. In this case, if we assume that the entire accumulated store of fuel is used up during a burst, then the total energy released during the burst increases with persistent flux from the system and, hence, with accretion rate.

Since the PCA spectrometer is not a telescope, i.e., the sky in the field of view of the instrument cannot be imaged, we cannot assert with confidence that precisely MX 0836-42 is the source of the detected bursts. Note, however, that only one known burster, MX 0836-42, was within the PCA field of view when each of the bursts was detected.

The RXTE observatory is in a low near-Earth orbit; therefore, its instruments can continuously monitor the source only during 65% of its 90-min orbit. Since more than one X-ray burst occurred in none of the PCA observing sessions that we used, we cannot reliably determine the burst recurrence time τ_R for MX 0836-42 from these data. However, in the two successive sessions on January 31, 2003, the PCA spectrometer detected two X-ray bursts separated by an interval of ~ 7205 s, which corresponds to the burst recurrence period determined for this source by Aoki et al. (1992). The source was continuously observed for ~ 2850 s after the first of these bursts; subsequently, the observations were interrupted for ~ 2610 s and then resumed. The 3-20 keV flux averaged over the second of the bursts was $F = (3.50 \pm 0.81) \times 10^{-9} \text{ erg cm}^{-2} \text{ s}^{-1}$, and the mean integrated flux from the source in the energy range 3-120 keV between these bursts was $F = (1.61 \pm 0.06) \times 10^{-9} \text{ erg cm}^{-2} \text{ s}^{-1}$. We assume that the bulk of the radiative energy during the burst is released in the range 3-20 keV.

In accordance with the current understanding of the burster phenomenon, the gravitational energy E_g of the matter accreted by the neutron star is released between X-ray bursts from such a system and the energy E_b of its thermonuclear burning is released during bursts. If we assume that no other bursts occurred over the interval between the pointings containing the first and second bursts during which the system was not monitored, then we can determine the thermonuclear burning parameter, the ratio $\alpha = \frac{E_g}{E_b}$, from the relationship

$$\alpha \approx \tau_R L_P / \tau_B L_B, \tag{1}$$

where $L_P = 1.24 \times 10^{37} (D/8kpc)^2 \text{ erg s}^{-1}$ and $L_B = 5.04 \times 10^{37} (D/8kpc)^2 \text{ erg s}^{-1}$ are the mean persistent and burst luminosities of the system and $\tau_B = 12.3$ s and $\tau_R = 7205$ s are the second burst duration and the period between bursts, respectively. In our case, formula (1) yields $\alpha \approx 144$, typical of a burst occurring through helium detonation (Bildsten 2000).

If we assume that the regime of thermonuclear burning did not change from burst to burst, then we can estimate the burst recurrence periods in other sessions using the above value

of α . Table 5 gives the burst recurrence times for the source under study determined using formula (1) by assuming that $\alpha \approx 140$. Comparison between the recurrence periods and the mean duration of the source’s continuous monitoring by the observatory lets the fact of observation of only one burst in each of the sessions can be easily explained. It is worth mentioning that the estimates obtained by this method are a factor of 2-3 larger than the burst recurrent period for MX 0836-42 determined by Aoki et al. (1992): $\tau_R \sim 2$ h. If we assume that $\tau_R \sim 2$ h, then we can determine the parameter $\alpha \sim 80$ averaged over all of the observed bursts using formula (1); this value is typical of mixed hydrogen helium bursts (Bildsten 2000). This model describes better the shape of the observed bursts, in particular, the relatively long (6-8 s) period of the burst rise to its maximum level.

Table 2 gives the accretion rate corresponding to the detected persistent integrated flux from the source under study and the corresponding recurrence periods of hydrogen helium bursts from it calculated by assuming that accreted matter occupies 1/3 of the surface (τ_1) and the entire surface (τ_2) of the neutron star. We see from this table that if the bursts in MX 0836-42 are hydrogen helium ones, then the accreted matter involved in the explosion during the burst occupies only part of the neutron star surface.

DISCUSSION

Figure 2 shows the light curve for MX 0836-42 constructed from all of the available ASM data, in which we clearly see a rise in the flux from the source on a time scale of ~ 600 days. Clearly, even if this phenomenon is periodic, the period of such bursts is more than 7 years. For example, nonuniformity in the accretion process can be responsible for such bursts.

It follows from Fig. 3 that there is a group of three observations with an anomalously high absorption level among the RXTE observations of the source (Table 3). It can be assumed that additional absorption possibly associated with the outer regions of the accretion disk appears in the system during these observations. The following fact argues for this explanation: the harder (more absorbed) the spectrum, the stronger the iron emission line in it. For example, the line equivalent width in the spectrum constructed from the observations on January 26 was ~ 120 eV, while this parameter for the 29₁ observations was ~ 310 eV. This explanation suggests a large inclination of the accretion disk in the system under study. This process can be periodic and related to the orbital motion in the binary system; i.e., the source can be a dipper. To test this assumption, we analyzed the light curve of the source in the energy range 1.3-3.0 keV, which is subject to the strongest absorption, constructed from the ASM/RXTE data for the period from January 5, 1996, through April 7, 2005, for the presence of periodic variations in the frequency range $(5 - 300) \times 10^{-6}$ Hz, which is typical of the orbital motion of a low-mass binary. This analysis failed to reveal any significant period of the signal variations.

The transient X-ray pulsar GRS 0834-43 is in the immediate vicinity of the source under study (24 arcmin). Since the PCA and HEXTE spectrometers are incapable of spatially resolving the sources of the detected emission, the above pulsar could introduce distortions

in the observed spectrum of MX 0836-42 when falling within the fields of view of these instruments. To test this hypothesis, we searched for the pulsations with a period of ~ 12 s that are typical of the pulsar GRS 0834-43 using all the available PCA observations of MX 0836-42. These studies failed to reveal any pulsating component whose confidence level would exceed 3σ in any of the observations. It is worth mentioning that the ASM/RXTE data revealed no flare activity in the emission from GRS 0834-43 during the period under consideration, while according to the ISGRI/IBIS data, the confidence level of the source's detection in the range 20-60 keV from January 2003 through March 2004 did not exceed 3σ ; the upper limit on the flux from the source was 1 mCrab throughout this period and ~ 10 mCrab for the period of a single observation (~ 2 ks). Thus, we can state the persistent spectra constructed from the available PCA and HEXTE data actually pertain to MX 0836-42.

In the course of some of the 15 X-ray bursts detected by the PCA spectrometer during the pointings at the source under study, the mean color radius of the emitting object was 4-7 km (Figs. 5c and 5d), which is smaller than the value obtained in terms of the standard models for the structure of a neutron star for its radius. A modification of the source's spectrum through scattering, which leads to an overestimation of the color temperature and an underestimation of the color radius (London et al. 1986; Sunyaev and Titarchuk 1986; Babul and Paczynski 1987), could be responsible for this discrepancy.

We see from Table 5 that the total energy released during the burst on January 31₂, 2003, is a factor of 2-3 lower than that for the remaining bursts, and that the burst itself occurred a factor of 2 earlier than the accumulation of a matter column density enough for detonation could occur (if detonation affects the entire surface of the neutron star) (Table 2). A similar situation was observed in the emission from this source on February 18, 1991 (Aoki et al. 1992), except that the separation between the bursts in that case was only ~ 10 min. These phenomena can be explained as follows:

- (1) Another burster is the burst source. Although this burst is morphologically similar to other bursts from the source under consideration, given that the PCA spectrometer is incapable of imaging the observed sky region, this assumption cannot be refuted using the available data. This assumption can also explain the different maximum burst energy fluxes from the source.
- (2) The thermonuclear burning during the burst proceeds in a regime different from the remaining cases. This is possible if, for example, some amount of fuel was not used up during a previous burst. In cases 1 and 2, we can say nothing about the parameter α and the burst recurrent period in other sessions.
- (3) Accretion affected a smaller part of the neutron star surface, which led to a faster accumulation of matter to the column density required for detonation. This could be evidenced by the larger increase in the color radius at the burst onset and its larger decrease at the burst end than those for other bursts (Fig. 5d).

ACKNOWLEDGMENTS

We thank M.G. Revnivtsev for valuable suggestions and remarks made by him when preparing this paper. This work is based on the observational data obtained by the INTEGRAL observatory and provided through the Russian and European INTEGRAL Science Data Centers as well as the data obtained by the RXTE observatory and provided through the NASA's HEASARC Web page on the Internet (<http://legacy.gsfc.nasa.gov>). This study was supported by the Russian Foundation for Basic Research (project no. 05-02-17454), the Presidium of the Russian Academy of Sciences (the Nonstationary Astronomical Phenomena Program), and the Program for Support of Leading Scientific Schools (project no. NSh-2083.2003.2).

- Aoki et al. 1992 (T. Aoki, T. Dotani, K. Ebisawa, et al.), *Publ. Astron. Soc. Japan* 44, 641 (1992).
- Babul and Paczynski 1987 (A. Babul, B. Paczynski), *Astrophys. J.* 323, 582 (1987).
- Basinska et al. 1984 (E. M. Basinska, W. H. G. Lewin, M. Sztajno, et al.), *Astrophys. J.* 281, 337 (1984).
- Belloni et al. 1993 (T. Belloni, G. Hasinger, W. Pietech, et al.), *Astron. Astrophys.* 271, 487 (1993).
- Bildsten 2000 (L. Bildsten), 2000arXt.confE.65B
- Cominsky et al. 1978 (L. Cominsky, C. Jones, W. Forman, H. Tananbaum), *Astrophys. J.* 224, 46 (1978).
- Eismont et al. 2003 (N.A. Eismont, A. V. Ditrikh, G. Janin, et al.), *Astron. Astrophys.* 411, L37 (2003).
- Grebenev and Sunyaev 1991 (S. Grebenev, R. Sunyaev), *IAU Circ.* 5294 (1991).
- Hasinger et al. 1990 (G. Hasinger, W. Pietsch, T. Belloni), *IAU Circ.* 5142 (1990).
- Kellogg et al. 1971 (E. Kellogg, H. Gursky, S. Murray, et al.), *Astrophys. J. Lett.* 169, L99 (1971).
- Lapshov et al. 1992 (I. Yu. Lapshov, V. V. Dremin, R. A. Sunyaev, et al.), *Pis'ma Astron Zh.* 18, 30 (1992) [*Sov. Astron. Lett.* 18, 12 (1992)].
- Lund et al. 2003 (N. Lund, S. Brandt, C. Budtz-Joergesen, et al.), *Astron. Astrophys.* 411, 231 (2003).
- Lewin and Joss 1981 (W. H. G. Lewin, P. C. Joss), *Space Sci. Rev.* 28, pp.3-87 (1981).
- Lewin et al. 1980 (W. H. G. Lewin, J. van Paradijs, L. Cominsky, S. Holzner), *MNRAS* 193, 15 (1980).
- Makino 1990 (F. Makino), *IAU Circ.* 5139 (1990).
- Markert et al. 1975 (T. Markert; H.V. Bradt; Clark, G.W., et al.), *IAU Circ.* 2765 (1975).
- Markert et al. 1977 (T. Markert, C.R. Canizares, G.W. Clark, et al.), *Astrophys. J.* 218, 801 (1977).
- Murakami et al. 1980 (T. Murakami, H. Inoue, K. Koyama, et al.), *Astrophys. J.* 240, 143 (1980).
- Sunyaev et al. 1990, *IAU Circ.* 5122 (1990).
- Sunyaev 1991, *IAU Circ.* 5180 (1991).
- Sunyaev and Titarchuk 1986 (R. Sunyaev, L. Titarchuk), *Pis'ma Astron Zh.* 12, 857 (1986).
- Sztajno et al. 1983 (M. Sztajno, E. M. Basinska, L. R. Cominsky, et al.), *Astrophys. J.* 267, 713 (1983).
- Ubertini et al. 2003 (P. Ubertini, F. Lebrun, G. Di Cocco, et al.), *Astron. Astrophys.* 411, 131 (2003).
- Winkler et al. 2003 (C. Winkler, T.J.-L. Courvoisier, G. Di Cocco, et al.), *Astron. Astrophys.* 411, L1 (2003).

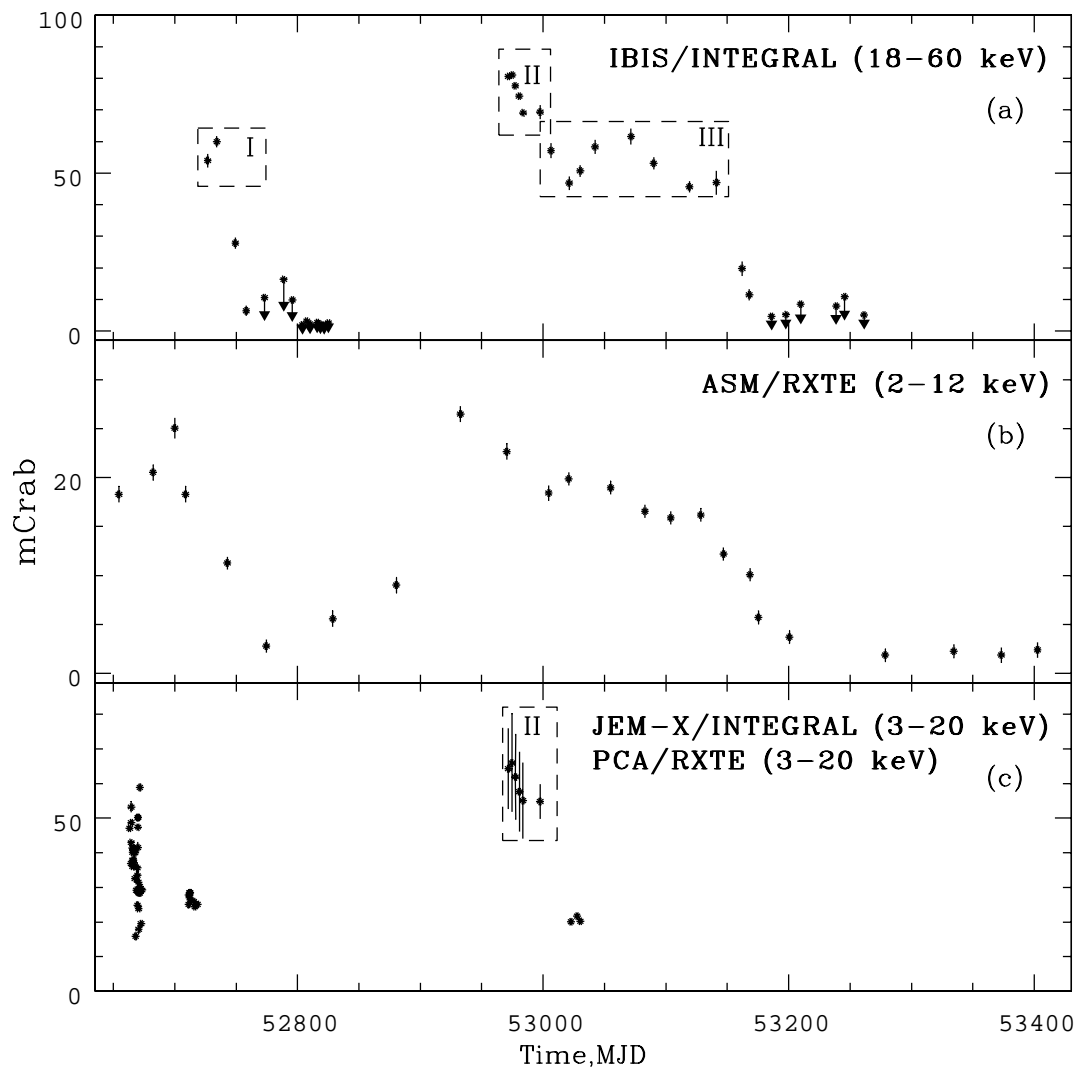


Fig. 1: Light curves for MX 0836-42 constructed from (a) ISGRI/IBIS/INTEGRAL data, (b) ASM/RXTE data, and (c) PCA/RXTE and JEM-X/INTEGRAL data (region II). The upper limits on the flux are given at the 3σ level.

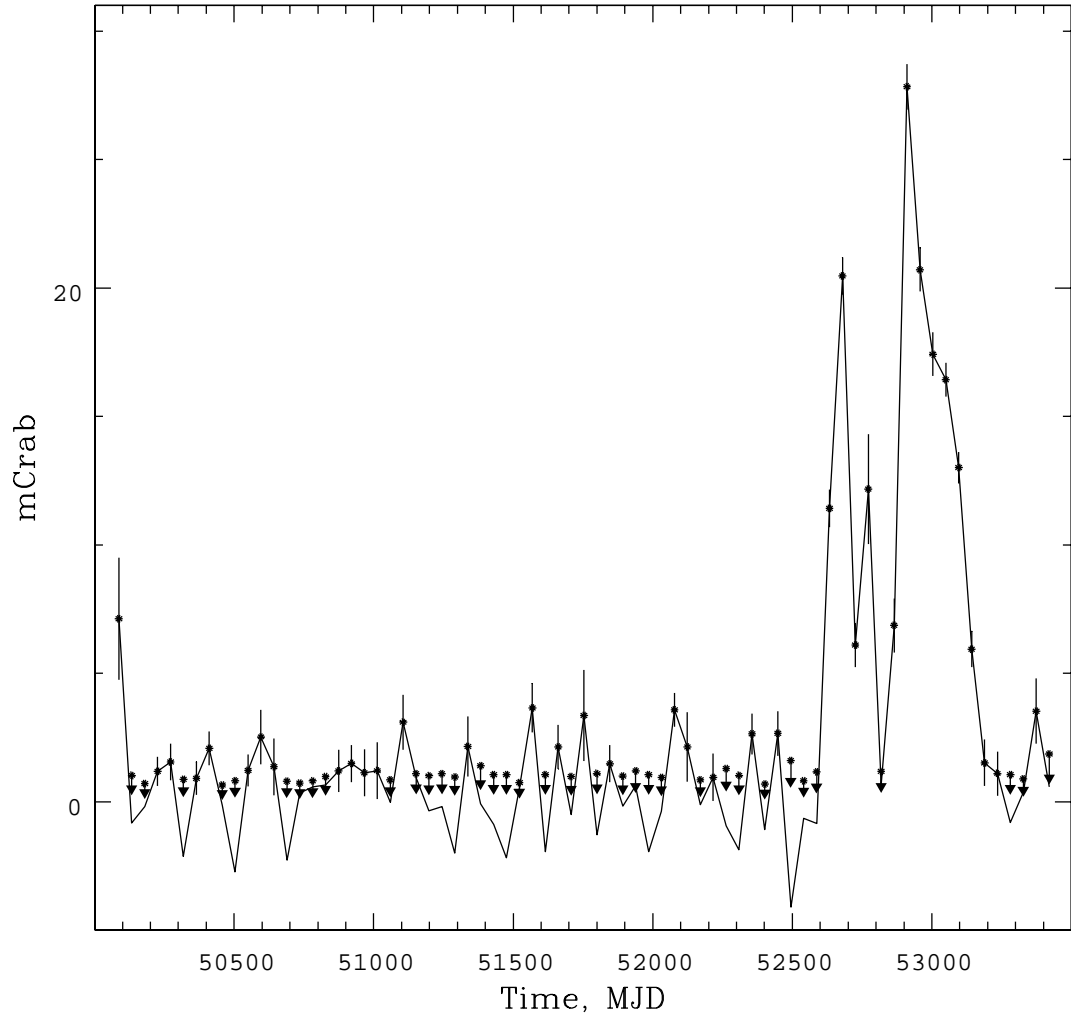


Fig. 2: Light curve for MX 0836-42 in the energy range 2-12 keV constructed from ASM/RXTE data.

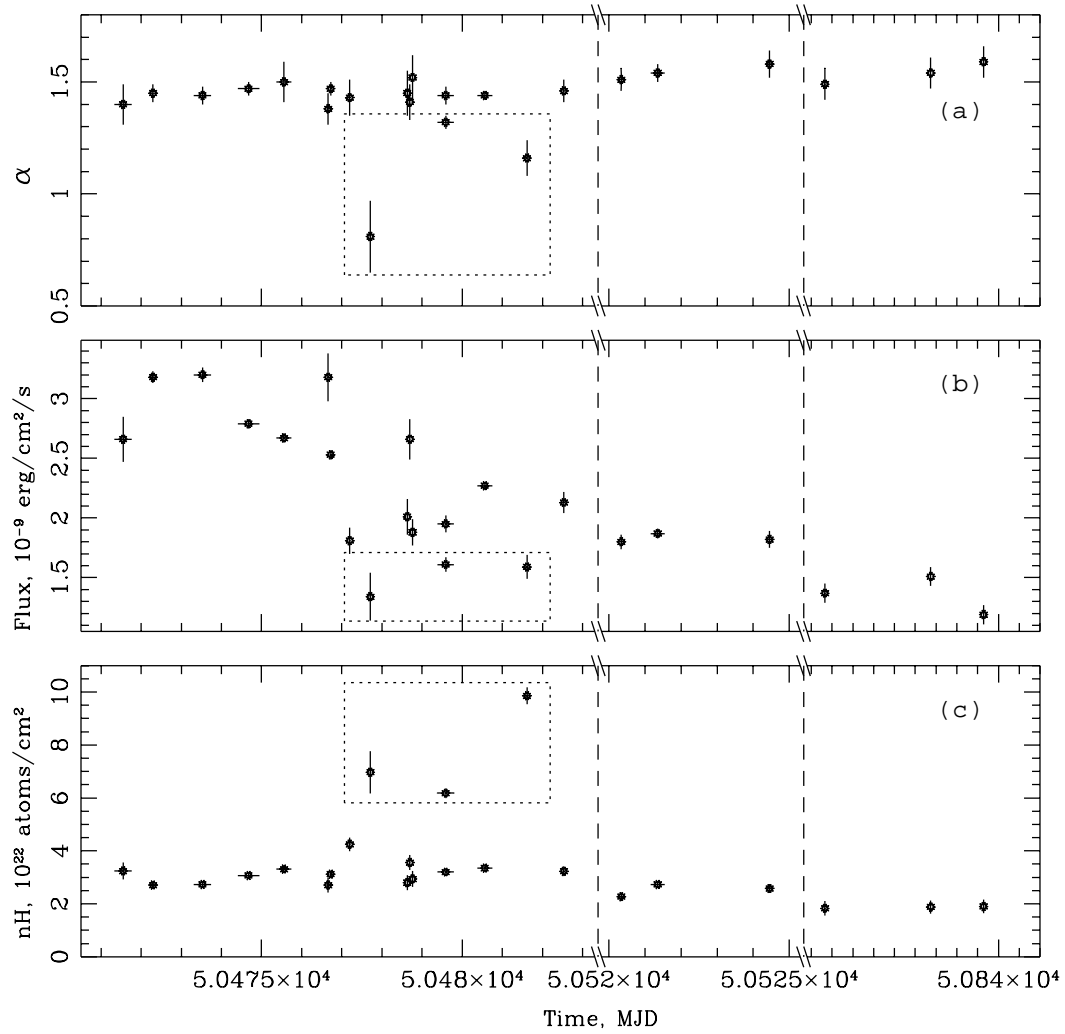


Fig. 3: (a) Time dependences of the photon index, (b) the 3-120 keV flux, and (c) the interstellar absorption derived from the RXTE (PCA+HEXTE) observations of MX 0836-42 in 2003-2004.

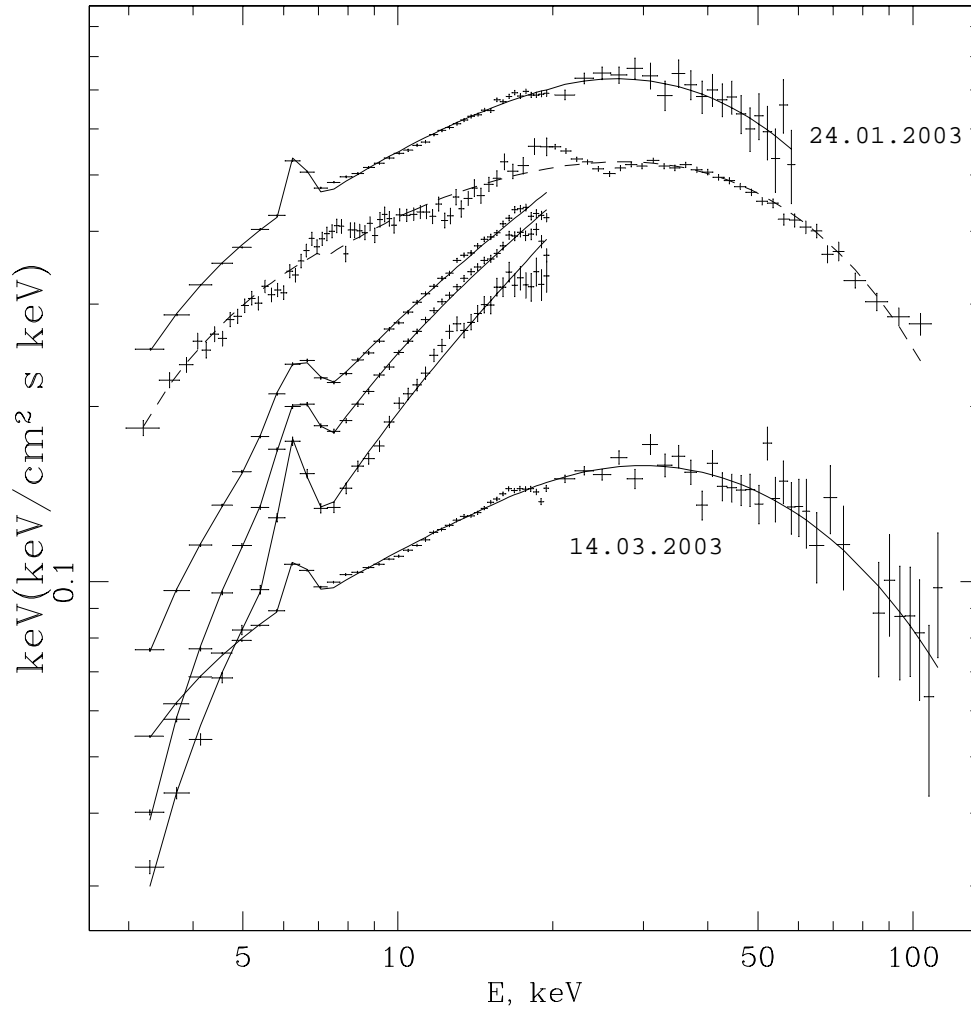


Fig. 4: Persistent spectra for MX 0836-42 constructed from the data of the JEM-X and ISGRI/IBIS telescopes aboard the INTEGRAL observatory (dashed line) and the PCA (3-20 keV) and HEXTE (20-60 keV) detectors aboard the RXTE observatory (solid lines). For convenience of perception, the values of these spectra and the model in the spectrum for March 14, 2003, were multiplied by a factor of 1/3.

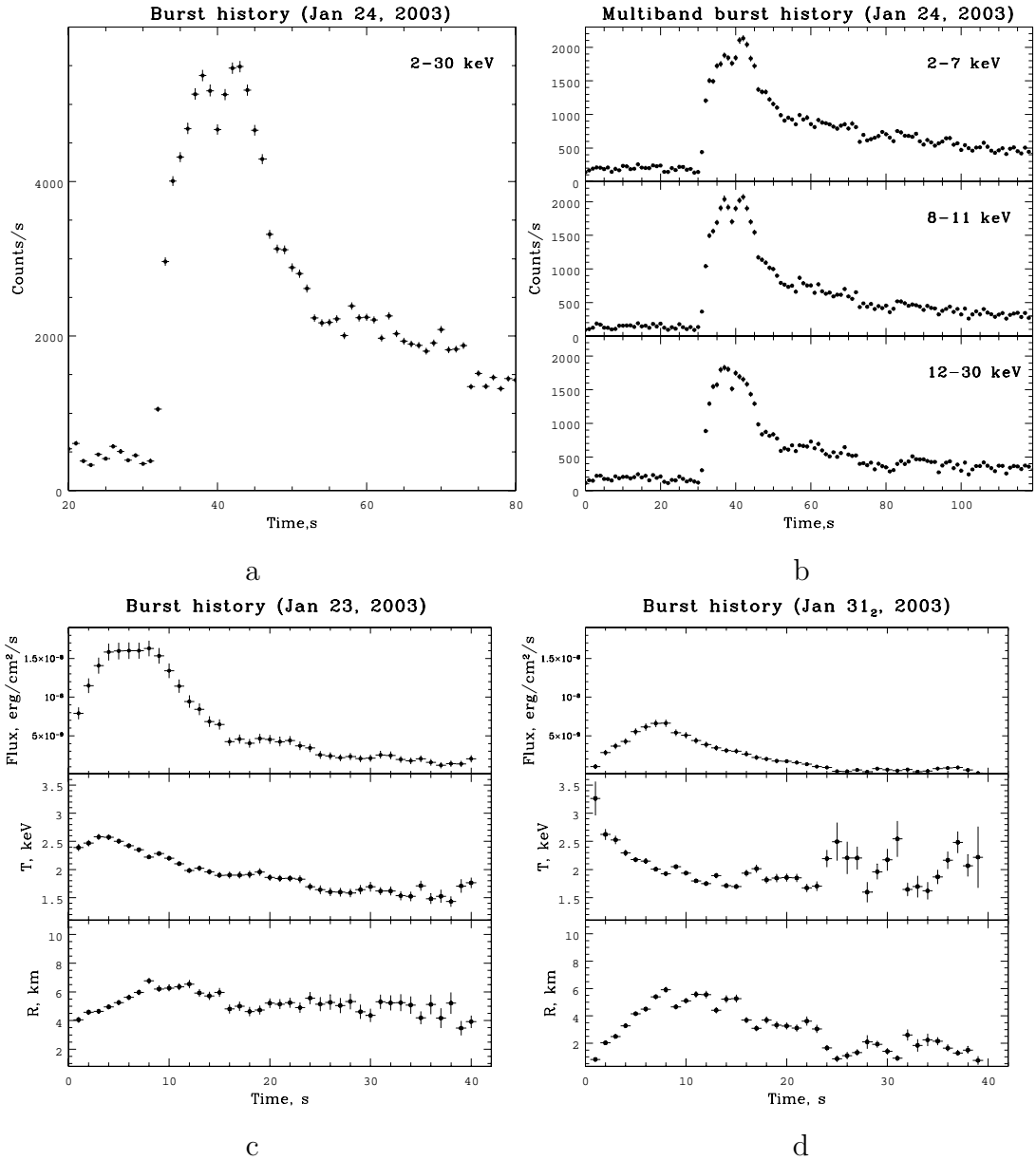


Fig. 5: Panels (a) and (b) show the time histories of the burst detected on January 24, 2003, from MX 0835-42 by the PCA/RXTE spectrometer in various energy ranges. A double-peaked structure of the burst near the maximum is clearly seen. Panels (c) and (d) display the time dependences of the 3-20 keV flux and the temperature and radius of the emitting object determined by fitting the spectra of MX 0836-42 by a blackbody during the bursts detected in 2003-2004 by PCA/RXTE. The time in panels (c) and (d) is measured from the burst onset; in panels (a) and (b), the burst onset corresponds to 30 s on the time axis.

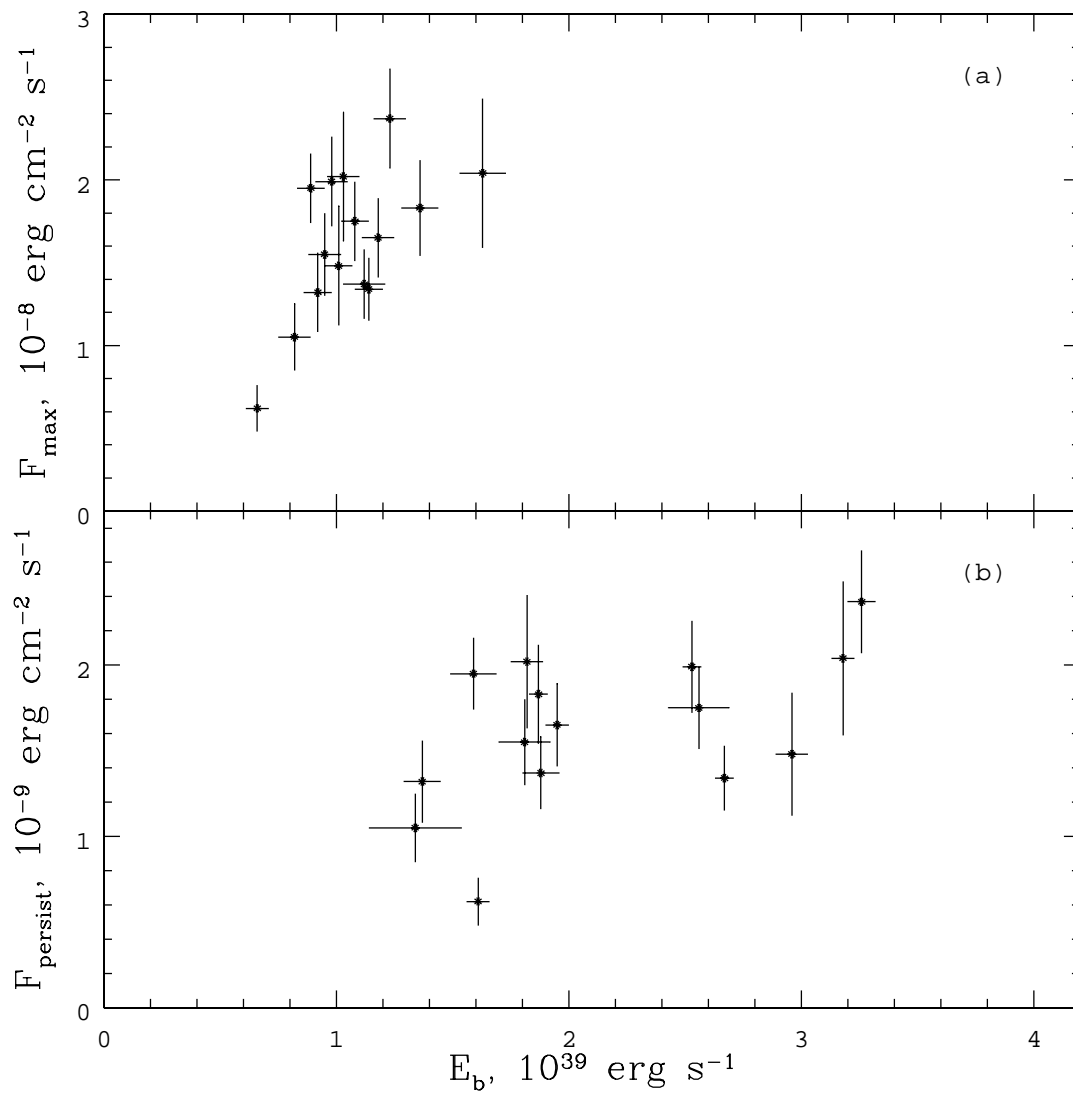


Fig. 6: (a) Maximum burst flux versus total energy released during the burst and (b) persistent flux from the source vs. total energy released during the burst. The dependences were constructed for the 15 X-ray bursts detected from MX 0836-42 using PCA/RXTE data.

Table 1: Observations of MX 0836-42 by the JEM-X and IBIS telescopes of the INTEGRAL orbiting observatory

Beginning of observation, UTC	End of observation, UTC	Exposure IBIS, s	Exposure JEM-X, s	Flux ISGRI/IBIS (20-120 keV), mCrab
2003				
28.03	<i>Mar</i> 28	6571	–	53.94 ± 2.16
05.04	<i>Apr</i> 5	6600	–	59.95 ± 1.77
20.04	<i>Apr</i> 20	6600	–	27.85 ± 1.76
29.04	<i>Apr</i> 29	6713	4513	6.45 ± 1.68
14.05	<i>May</i> 14	8802	4399	10.60 ^a
29.05	<i>May</i> 29	6600	2200	16.30 ^a
05.06	<i>Jun</i> 5	8917	2201	9.84 ^a
12.06	<i>Jun</i> 15	202879	93575	1.95 ^a
16.06	<i>Jun</i> 18	142958	94976	3.13 ± 0.39
19.06	<i>Jun</i> 21	193103	88973	2.24 ^a
26.06	<i>Jun</i> 27	106271	85499	2.66 ^a
28.06	<i>Jun</i> 30	192907	122629	2.05 ^a
01.07	<i>Jul</i> 3	175646	145142	1.95 ^a
04.07	<i>Jul</i> 6	113051	98261	2.60 ^a
27.11	<i>Nov</i> 29	206101	54131	80.56 ± 0.38
30.11	<i>Dec</i> 2	206942	113931	81.12 ± 0.32
03.12	<i>Dec</i> 5	186043	97123	77.59 ± 0.35
06.12	<i>Dec</i> 8	207723	88880	74.39 ± 0.33
09.12	<i>Dec</i> 11	193980	98270	69.01 ± 0.32
24.12	<i>Dec</i> 24	6714	4514	69.37 ± 2.22
2004				
02.01	<i>Jan</i> 2	4463	2263	57.17 ± 2.39
17.01	<i>Jan</i> 17	5713	3513	46.81 ± 2.13
26.01	<i>Jan</i> 26	6602	2201	50.69 ± 1.88
07.02	<i>Feb</i> 7	6634	–	58.36 ± 2.21
07.03	<i>Mar</i> 7	4388	–	61.62 ± 2.55
26.03	<i>Mar</i> 26	6626	–	53.14 ± 1.88
24.04	<i>Apr</i> 24	6712	4512	45.69 ± 1.79
16.05	<i>May</i> 16	2314	–	46.95 ± 3.83
06.06	<i>Jun</i> 6	4400	–	19.78 ± 2.34
11.06	<i>Jun</i> 11	6602	2201	11.51 ± 1.82
30.06	<i>Jun</i> 30	8123	2200	4.62 ^a
11.07	<i>Jul</i> 11	6602	2200	5.17 ^a
23.07	<i>Jul</i> 23	4401	–	8.49 ^a
21.08	<i>Aug</i> 21	5470	–	7.95 ^a
28.08	<i>Aug</i> 28	2221	–	10.83 ^a
13.09	<i>Sep</i> 13	8064	2171	5.14 ^a

Note. Exposure is the total duration of all pointings during which the source was resolved.

^a - 3σ is an upper limit on the energy flux from the source.

Table 2: Observations of MX 0836-42 by the PCA and HEXTE instruments of the RXTE orbiting observatory

Date, UTC	Exposure ^a PCA	Exposure ^a HEXTE	$\dot{M}^b \times 10^{-9}$, M_{\odot}/yr	τ_1^c , s	τ_2^d , s
2003					
23.01	11296	5539	2.08 ± 0.03	3230	9680
24.01	5088	2268	2.09 ± 0.04	3180	9810
25.01	10592	5689	1.82 ± 0.03	3640	10930
26.01	14144	7506	1.75 ± 0.02	3810	11420
27.01	9504	5189	1.65 ± 0.03	4020	12060
28 ₁ .01	1872	721	2.08 ± 0.12	3200	9580
28 ₂ .01	864	294	1.18 ± 0.08	5620	16870
29 ₁ .01	1744	602	0.88 ± 0.12	7560	22680
29 ₂ .01	944	393	1.31 ± 0.05	5070	15200
30 ₁ .01	896	367	1.74 ± 0.05	3820	11450
30 ₂ .01	736	327	1.23 ± 0.05	5410	16220
30 ₃ .01	720	318	1.74 ± 0.06	3820	11460
31 ₁ .01	5520	2253	1.28 ± 0.05	5170	15510
31 ₂ .01	4032	2128	1.05 ± 0.04	6340	19020
01.02	8992	5085	1.48 ± 0.07	4710	13460
02.02	2944	1413	1.04 ± 0.06	6400	19200
03.02	2464	1007	1.39 ± 0.06	4780	14340
13.03	4672	2211	1.18 ± 0.04	5620	16870
14.03	10496	5029	1.22 ± 0.02	5300	15900
17.03	3360	1627	1.23 ± 0.05	5400	16200
18.03	3392	1583	1.12 ± 0.05	5930	17190
20.03	3472	1652	1.19 ± 0.05	5590	16750
2004					
18.01	1120	464	0.90 ± 0.47	4990	14960
23.01	1216	520	0.99 ± 0.03	5040	15110
26.01	1552	723	0.78 ± 0.02	6390	19160

Note. The subscript in the dates indicate the pointing number during the corresponding day.

^a - The total exposure time in seconds.

^b - The accretion rate.

^c - The burst recurrence period calculated in the case where 1/3 of the neutron star surface is covered with accreted matter.

^d - The burst recurrence period calculated in the case where the neutron star surface is completely covered with accreted matter.

Table 3: Results of fitting the RXTE (PCA+HEXTE) spectra of MX 0836-42 by a power law with a high-energy exponential cutoff with allowance made for the interstellar absorption and the iron emission line at $E_{Fe} = 6.4$ keV and the reflection of emission from the accretion disk

Date, UTC	α^a	E_{cut}^b , keV	Flux ^c , erg/cm ² /s	N_H^d , 10 ²² at./cm ²	K^e	$\chi^2(N)^f$
2003						
23.01	1.45 ± 0.04	53.9 ± 4.9	3.18 ± 0.05	2.71 ± 0.08	0.75	1.27(60)
24.01	1.44 ± 0.04	45.9 ± 4.6	3.20 ± 0.06	2.73 ± 0.09	1.00	0.87(66)
25.01	1.47 ± 0.03	53.3 ± 3.8	2.79 ± 0.04	3.07 ± 0.06	0.74	1.16(63)
26.01	1.50 ± 0.09	67.4 ± 3.8	2.67 ± 0.04	3.31 ± 0.07	0.79	2.08(50)
27.01	1.47 ± 0.03	57.9 ± 3.1	2.53 ± 0.04	3.12 ± 0.08	0.76	1.09(59)
28 ₁ .01	1.38 ± 0.07	50.6 ± 10.1	3.18 ± 0.20	2.71 ± 0.28	1.03	0.87(51)
28 ₂ .01	1.43 ± 0.08	38.2 ± 7.7	1.81 ± 0.11	4.25 ± 0.26	0.57	0.97(52)
29 ₁ .01	0.81 ± 0.16	29.4 ± 4.6	1.34 ± 0.20	6.97 ± 0.79	0.77	1.99(52)
29 ₂ .01	1.45 ± 0.10	43.7 ± 14.7	2.01 ± 0.15	2.80 ± 0.29	0.93	0.88(44)
30 ₁ .01	1.41 ± 0.08	45.8 ± 8.2	2.66 ± 0.17	3.56 ± 0.28	0.97	0.91(52)
30 ₂ .01	1.52 ± 0.10	50.0(<i>fixed</i>)	1.88 ± 0.11	2.94 ± 0.30	1.12	1.05(53)
30 ₃ .01	1.40 ± 0.09	56.1 ± 14.4	2.66 ± 0.19	3.24 ± 0.32	0.98	0.93(49)
31 ₁ .01	1.44 ± 0.04	50.3 ± 5.3	1.95 ± 0.07	3.20 ± 0.11	0.75	1.25(52)
31 ₂ .01	1.32 ± 0.03	43.5 ± 4.1	1.61 ± 0.06	6.18 ± 0.19	0.70	1.88(52)
01.02	1.44 ± 0.02	61.0 ± 3.8	2.27 ± 0.03	3.35 ± 0.07	0.54	1.27(66)
02.02	1.16 ± 0.08	35.3 ± 3.4	1.59 ± 0.10	9.86 ± 0.32	0.87	1.29(50)
03.02	1.46 ± 0.05	53.4 ± 7.9	2.13 ± 0.09	3.23 ± 0.19	0.90	1.03(52)
13.03	1.51 ± 0.05	65.8 ± 8.3	1.80 ± 0.06	2.27 ± 0.16	0.71	1.27(55)
14.03	1.54 ± 0.04	64.9 ± 5.5	1.87 ± 0.04	2.73 ± 0.09	0.76	1.08(50)
17.03	1.54 ± 0.06	76.2 ± 12.6	1.88 ± 0.08	2.33 ± 0.20	0.86	0.88(55)
18.03	1.51 ± 0.06	67.5 ± 12.4	1.71 ± 0.08	2.46 ± 0.21	0.81	0.98(52)
20.03	1.58 ± 0.06	71.4 ± 14.1	1.82 ± 0.07	2.58 ± 0.17	0.92	0.87(48)
2004						
18.01	1.49 ± 0.07	50.0(<i>fixed</i>)	1.37 ± 0.08	1.83 ± 0.28	1.01	0.96(54)
23.01	1.54 ± 0.07	50.0(<i>fixed</i>)	1.51 ± 0.08	1.88 ± 0.25	0.98	0.93(54)
26.01	1.59 ± 0.07	53.5 ± 15.2	1.19 ± 0.08	1.90 ± 0.26	0.65	1.27(53)

^a - The photon index.

^b - The exponential cutoff energy.

^c - The persistent (3-120 keV) flux from the source ($\times 10^{-9}$ erg cm⁻² s⁻¹)

^d - The hydrogen column density obtained when fitting the spectrum.

^e - The scaling factor of the HEXTE spectrum.

^f - The χ^2 value of the best fit to the spectrum normalized to the number of degrees of freedom N.

Table 4: X-ray bursts detected from MX 0836-42 by the JEM-X instrument of the INTEGRAL orbiting observatory

Date ^a , MJD	F_m^b , Crab	Date ^a , MJD	F_m^b , Crab	Date ^a , MJD	F_m^b , Crab
52971.954857	0.83 ± 0.20	52975.559510	0.75 ± 0.20	52980.954001	0.72 ± 0.18
52972.054063	0.62 ± 0.15	52977.293263	0.85 ± 0.21	52981.048922	0.74 ± 0.19
52972.158769	0.93 ± 0.22	52977.465705	0.69 ± 0.17	52981.146508	0.63 ± 0.16
52973.403827	0.87 ± 0.21	52978.798908	0.85 ± 0.26	52981.242242	0.56 ± 0.17
52974.639704	0.76 ± 0.21	52979.840899	1.12 ± 0.24	52982.428908	0.51 ± 0.16
52974.733813	0.69 ± 0.19	52979.930894	0.77 ± 0.17	52983.507589	0.57 ± 0.18
52975.372256	0.72 ± 0.24	52980.037844	0.84 ± 0.21	52983.710369	0.70 ± 0.17
52975.386177	0.55 ± 0.23	52980.124557	0.73 ± 0.18	52984.442369	0.85 ± 0.25

^a - The time the flux reaches its maximum.

^b - The maximum burst flux averaged over 1 s.

Table 5: X-ray bursts detected from MX 0836-42 by PCA aboard the RXTE observatory

Date, UTC	T^a , MJD	T_{exp}^b , s	T_{eff}^c , s	F_{max}^d , erg cm ⁻² s ⁻¹	F_p^e , erg cm ⁻² s ⁻¹	E_b^f , erg	τ_R^g , s
2003							
23.01	52662.593715	8.3	16.3	1.63 ± 0.10	3.18 ± 0.05	2.04 ± 0.45	11490
24.01	52663.305984	13.0	25.2	1.23 ± 0.07	3.26 ± 0.06	2.37 ± 0.30	13540
25 ₁ .01	52664.444097	17.3	21.2	1.08 ± 0.06	2.56 ± 0.13	1.75 ± 0.24	12500
25 ₂ .01	52664.630428	19.4	19.1	1.01 ± 0.06	2.96 ± 0.07	1.48 ± 0.36	9140
26.01	52665.702338	15.9	15.4	1.14 ± 0.06	2.67 ± 0.04	1.34 ± 0.19	9180
27.01	52666.560185	20.4	26.5	0.98 ± 0.07	2.53 ± 0.04	1.99 ± 0.27	14380
28.01	52667.668495	14.7	21.3	0.95 ± 0.07	1.81 ± 0.11	1.55 ± 0.25	15660
29.01	52668.191574	12.4	16.7	0.82 ± 0.07	1.34 ± 0.20	1.05 ± 0.20	14320
31 ₁ .01	52670.553704	12.6	18.3	1.18 ± 0.07	1.95 ± 0.05	1.65 ± 0.24	15470
31 ₂ .01	52670.637095	10.9	12.3	0.66 ± 0.05	1.61 ± 0.05	0.62 ± 0.14	7205
02.02	52672.624456	16.9	28.6	0.89 ± 0.06	1.59 ± 0.10	1.95 ± 0.21	22430
14.03	52712.408229	16.0	17.6	1.36 ± 0.08	1.87 ± 0.04	1.83 ± 0.29	17890
17.03	52715.453229	16.6	16.0	1.12 ± 0.09	1.88 ± 0.08	1.37 ± 0.21	13320
20.03	52718.536470	16.3	25.6	1.03 ± 0.07	1.82 ± 0.07	2.02 ± 0.39	20290
2004							
18.01	53022.663252	16.8	18.7	0.92 ± 0.06	1.37 ± 0.08	1.32 ± 0.24	17620

Note. The subscript in the dates indicates the burst number during the corresponding day.

^a - The burst onset time.

^b - The exponential burst decay time.

^c - The effective burst duration.

^d - The 3-20 keV maximum burst flux ($\times 10^{-8}$)

^e - The persistent 3-120 keV flux ($\times 10^{-9}$)

^f - The energy released during the burst ($\times (D/8 \text{ kpc})^2 \times 10^{39}$)

^g - The burst recurrence period (at $\alpha = 140$)